The first candidate for chiral nuclei in the $A \sim 80$ mass region: ^{80}Br

S.Y. Wang[a], B. Qi[a], L. Liu[a], S.Q. Zhang[*,b], H. Hua[b], X.Q. Li[b], Y.Y. Chen[b], L.H. Zhu[c], J. Meng[*,b,c,d], S.M. Wyngaardt[d], P. Papka[d], T.T. Ibrahim[d,e,f], R.A. Bark[e], P. Datta[e], E.A. Lawrie[e], J.J. Lawrie[e], S.N.T. Majola[e], P.L. Masiteng[e], S.M. Mullins[e], J. Gál[g], G. Kalinka[g], J. Molnár[g], B.M. Nyakó[g], J. Timár[g], K. Juhász[h], R. Schwengner[i]

[a] *Shandong Provincial Key Laboratory of Optical Astronomy and Solar-Terrestrial Environment, School of Space Science and Physics, Shandong University at Weihai, Weihai 264209, China*

[b] *State Key Lab Nucl. Phys. & Tech., School of Physics, Peking University, Beijing 100871, China*

[c] *School of Physics and Nuclear Energy Engineering, Beihang University, Beijing 100191, China*

[d] *Department of Physics, University of Stellenbosch, Matieland 7602, South Africa*

[e] *iThemba LABS, 7129 Somerset West, South Africa*

[f] *Department of Physics, University of Ilorin, PMB 1515, Ilorin, Nigeria*

[g] *Institute of Nuclear Research of the Hungarian Academy of Sciences (ATOMKI), H-4001 Debrecen, P.O.Box: 51, Hungary*

[h] *Department of Information Technology, University of Debrecen, Egyetem tér 1, Debrecen, Hungary*

[i] *Institut für Strahlenphysik, Helmholtz-Zentrum Dresden-Rossendorf, D-01314 Dresden, Germany*

Abstract

Excited states of ^{80}Br have been investigated via the ^{76}Ge(^{11}B, α3n) and ^{76}Ge(^{7}Li, 3n) reactions and a new $\Delta I = 1$ band has been identified which resides $\sim$ 400 keV above the yrast band. Based on the experimental results and their comparison with the triaxial particle rotor model calculated ones, a chiral character of the two bands within the $\pi g_{9/2} \otimes \nu g_{9/2}$ configuration is proposed, which provides the first evidence for chirality in the $A \sim 80$ region.

*Corresponding author

Email addresses: sqzhang@pku.edu.cn (S.Q. Zhang), mengj@pku.edu.cn (J. Meng)

Key words: high-spin states, chirality, particle rotor model, ^{80}Br
PACS: 21.60.Ev, 21.10.Re, 23.20.Lv

1. Introduction

The spontaneously broken chiral symmetry is a well-known phenomenon in chemistry, biology and particle physics. Recently, this phenomenon in atomic nuclei has attracted significant attention and intensive discussion.

The first prediction of chiral effects in atomic nuclei was made by Frauendorf and Meng in 1997 [1]. They pointed out that the rotation of triaxial nuclei may give rise to pairs of identical ΔI=1 bands with the same parity, which are called chiral doublet bands [1]. Presently, candidates for chiral doublet bands have been observed experimentally in about 25 cases of odd-odd nuclei, odd-A and even-even nuclei (see review [2, 3] and references therein). Thus far most studies on nuclear chirality have focused on the mass A ∼130 [4, 5, 6, 7, 8, 9, 10] and 100 [11, 12, 13] regions, although the explanations for some of them (e.g., ^{134}Pr and ^{104}Rh) are still under debate [11, 12, 14, 15, 16]. However, there is no reason to consider the nuclei in A ∼130 and 100 mass regions as unique in terms of the nuclear chirality. Recently, a pair of negative-parity partner bands in ^{198}Tl have been suggested as candidate chiral bands [17]. Thus, it is interesting to search for more candidates in other mass regions with the fingerprints for chirality in Refs. [3, 18] to show that these chiral symmetry properties are of a general nature and not related only to a specific nuclear mass region. Following the previous investigations, the experimental fingerprints for chirality established in A ∼100 and 130 mass regions, i.e., the near degeneracy of spectra, the similar $B(M1)$ and $B(E2)$ values, and the staggering of $B(M1)/B(E2)$ ratios, should be used for new mass region. Meanwhile the state of the art theoretical approach should be used to examine the triaxial deformation and the particle-hole configuration favorable for chirality.

Chiral rotation has also been predicted to occur in the A ∼80 mass region [19], where chiral doublet bands may be formed involving the $\pi g_{9/2} \otimes \nu g_{9/2}^{-1}$ configuration. For odd-odd Br isotopes with $A \sim 80$, the proton Fermi level ($Z = 35$) lies at the bottom of the $\pi g_{9/2}$ subshell, and with an increase of the neutron number N to the magic number 50, the neutron Fermi level approaches the top of the $\nu g_{9/2}$ subshell. Therefore, odd-odd Br isotopes with larger N are more suitable for sustaining chiral geometry than those

with smaller N, unless the value of N is close to magic number $N = 50$, where rotational structures are not easily developed.

Based on the above consideration, the odd-odd nucleus ^{80}Br may be considered as a good candidate for a chiral nucleus. Hence, it is interesting to populate high-spin states of the odd-odd nucleus ^{80}Br and to search for chiral doublet bands.

2. Experiments

High-spin states of ^{80}Br were populated using the fusion-evaporation reaction ^{76}Ge(^{11}B,α3n) at a beam energy of 54 MeV at the iThemba LABS in South Africa. The target consisted of a 1.8 mg/cm^2 ^{76}Ge metallic foil with 4.0 mg/cm^2 Au backing. The in-beam $\gamma-$rays were detected by the AFRODITE array [20], which consists of nine Compton-suppressed clover detectors. The clover detectors have been arranged in two rings at 90° and 135° with respect to the beam direction, hence the directional correlation of oriented (DCO) nuclei ratios for γ transitions can be extracted. In addition, the CsI particle detector array — Chessboard [21] was also used with the AFRODITE array to select specific reaction channels. A total of 2×10^8 $\gamma-\gamma$ coincidence events were accumulated. In order to double-check the experimental results, we have also used high-fold coincidence γ-ray data from a measurement of the reaction ^{7}Li + ^{76}Ge using an arrangement of six EUROBALL CLUSTER detectors [22]. In that experiment, approximately 1.2×10^9 coincidence events of fold 2 or higher were collected and sorted off-line into $E_\gamma - E_\gamma$ matrices as well as an $E_\gamma - E_\gamma - E_\gamma$ cube. The odd-odd nucleus ^{80}Br was produced as a by-product. More details on that experiment can be found in Ref. [23].

3. Result and Discussions

A partial level scheme of ^{80}Br derived from the present work and typical doubly gated coincidence spectra extracted from the cube are shown in Figs. 1 and 2, respectively. As shown in Fig. 1, the previously reported positive-parity band structures [24] have been considerably extended, and about 20 new transitions were added to the level scheme. The yrast band (labeled as Band 1) has been extended up to I^π=$(16)^+$. Note that a 1401-keV γ-ray instead of a 1348-keV one in Ref. [24] was assigned to transition $13^+ \rightarrow 11^+$ of the yrast band, which could be verified by the coincident relationship of

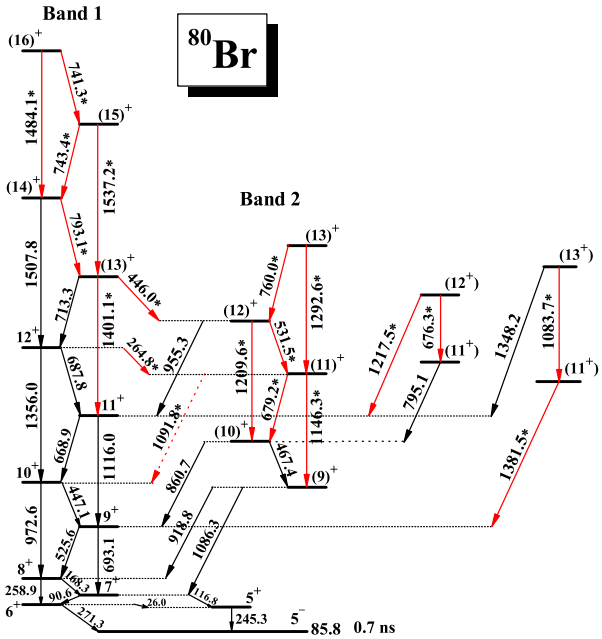

Figure 1: (color online) Partial level scheme for ^{80}Br obtained in the present work. New observed transitions are indicated by stars and red lines.

the 1401-keV γ-ray seen from Fig. 2(a). In addition, a new $\Delta I = 1$ positive-parity band structure (labeled as Band 2) was established up to spin (13^+). Remarkably, several linking transitions between the two bands, not only from band 2 to band 1 (such as 860.7 and 955.3 keV) but also from band 1 to band 2 (264.8 and 446.0 keV), were observed in the present work.

In the level scheme construction, we adopted the spins and parities for band 1 from Ref. [24] and determined the spins and parities of the other level sequences on the basis of the multipolarities of transitions connecting them to this band. The lowest energy state of band 2 decays by a 918.8-keV transition to the 8^+ and by a 1086.3-keV transition to the 7^+ state of band 1 (see Fig. 1). These two linking transitions had been reported in the previous work [24], where the 918.8-keV transition was assigned to be a $\Delta I = 1$ M1/E2 transition, and the 1086.3-keV transition was proposed to have $\Delta I = 2$ E2 or $\Delta I = 0$ M1/E2 multipolarities. According to the general yrast argument that levels populated in heavy-ion reactions usually have spins increasing with increasing excitation energy [25], we adopted the $\Delta I = 2$ E2 character for the 1086.3-keV transition. Thus the spin/parity assignment (9^+) has

been made for the lowest state of band 2. The multipolarity information on the 918.8- and 1086.3-keV transitions could be obtained accurately in the second experiment. In that experiment, with setting gates on stretched quadrupole transitions, the DCO ratios are ~ 1 for stretched quadrupole transitions and ~ 0.5 for pure dipole ones [23]. The present DCO ratios were extracted to be ~ 0.85 for the 1086.3-keV transition and ~ 0.38 for the 918.8-keV transition. This provides further support for the 9^+ assignment for the lowest state of band 2. Furthermore, when the γ transitions form rotational band structures, the cross-over transitions were set to have the E2 character, while the normal intra-band transitions were assumed to have M1/E2 nature. These arguments lead to the current spin-parity assignments shown in Fig. 1.

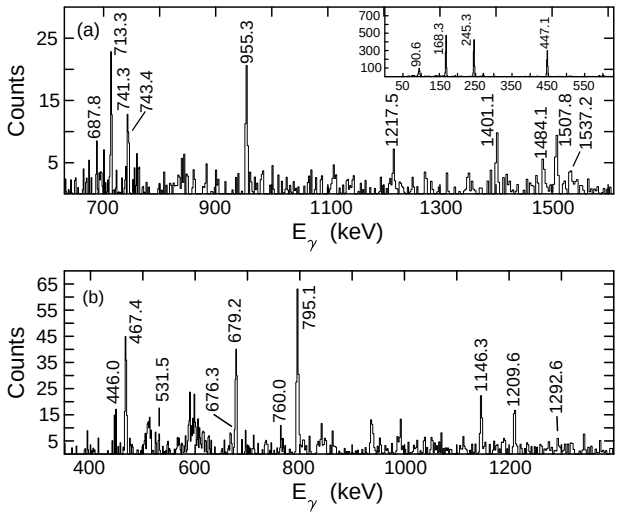

Figure 2: Background subtracted coincidence spectra, revealing the new transitions for band 1 (a) and band 2 (b) in ^{80}Br. The spectrum for band 1 is the sum of double gates: 1356.0&525.6 and 668.9&525.6 and the insert shows the low energy spectrum. The spectrum for band 2 is the sum of double gates: 918.8&168.3, 918.8&467.4, 918.8&1146.3, and 860.7&525.6.

Band 1 has been already assigned to the $\pi g_{9/2} \otimes \nu g_{9/2}$ configuration [24]. As shown in Fig. 1, band 2 has the same parity as the band 1. Furthermore, the existence of several M1/E2 and E2 linking transitions between the two bands indicates that band 2 has the same configuration $\pi g_{9/2} \otimes \nu g_{9/2}$ as that of the yrast band, as discussed in Refs. [4, 5, 9]. The degree of degeneracy of bands 1 and 2 in ^{80}Br is exhibited by the excitation energies as a function

of spin as shown in Fig. 3(a). The two bands maintain an energy difference around ∼400 keV within the observed spin interval. The experimental $B(\mathrm{M1})/B(\mathrm{E2})$ ratios are also extracted and presented in Fig. 4 for bands 1 and 2 in ^{80}Br. As shown in Fig. 4, the $B(\mathrm{M1})/B(\mathrm{E2})$ ratios for the two bands are comparable in magnitude, and in particular, the ratios for band 1 show clearly the odd-even staggering as a function of spin. Taking the experimental observations given above into account, bands 1 and 2 in ^{80}Br may be considered as candidates for chiral doublet bands, which had already been systematically reported in the odd-odd nuclei of A ∼100 mass region with $\pi g_{9/2} \otimes \nu h_{11/2}$ and of A ∼130 with $\pi h_{11/2} \otimes \nu h_{11/2}$. An interpretation of γ-vibration coupled to the yrast band is unlikely as the γ-vibration energies are larger than 600 keV in this mass region [26, 27].

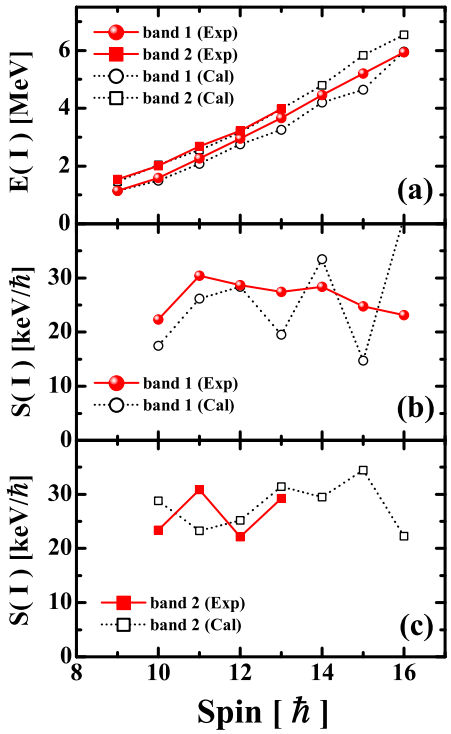

Figure 3: (color online) (a) Excitation energy and (b, c) staggering parameter S(I) = $[E(I) - E(I-1)]/2I$ as a function of spin for the doublet bands in ^{80}Br. The filled (open) symbols connected by solid (dotted) curves denote experimental (theoretical) values. The bands 1 and 2 are shown by circles and squares, respectively.

In the following, the calculations of the triaxial relativistic mean-field

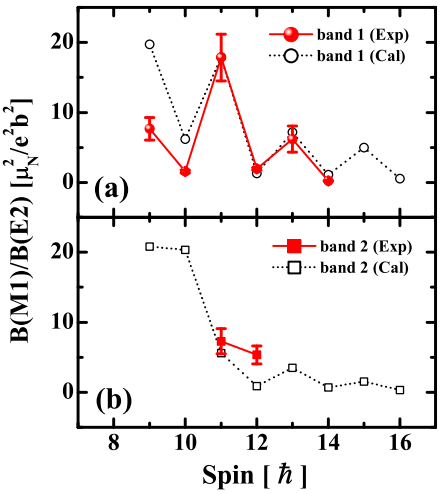

Figure 4: (color online) Comparisons of the measured and calculated in-band $B(M1)/B(E2)$ ratios for the bands 1 (a) and 2 (b) in ^{80}Br.

(RMF) theory [28] and the particle rotor model (PRM) [29, 30, 31] are used to discuss whether band 2 could be interpreted as chiral partner of band 1, and to investigate to the evolution of chiral geometry in this nucleus.

From the configuration-fixed constrained triaxial RMF calculations [28] with parameter set PK1 [32], the self-consistent deformation parameters β_2=0.346 and $\gamma = 24.59^\circ$ are obtained corresponding to the $\pi g_{9/2} \otimes \nu g_{9/2}$ configuration in ^{80}Br. These deformation parameters are suitable for the construction of chiral bands. Compared with the deformation values $\beta_2 \approx 0.2 - 0.3$ needed to reproduce the chiral doublet bands in $A \sim 100, 130$ mass region, the value β_2=0.346 is obviously much larger. It is noted that large quadrupole deformations of $\beta_2 \approx 0.3 - 0.4$ have been reported for the bands with $\pi g_{9/2} \otimes \nu g_{9/2}$ configuration in the lighter ^{74,76}Br nuclei [33, 34]. Lifetime measurements were carried out for the 10^+, 11^+ and 12^+ states in the yrast band of ^{80}Br in Ref. [24], and moderate quadrupole deformation parameters $\beta_2 = 0.17,\ 0.12$, and 0.12 were deduced respectively for these states with the assumption of the axial symmetry. If we turn to adopt the essential triaxiality $\gamma = 24.59^\circ$ from the RMF calculation, according to the procedure in Refs. [35, 36], a large quadrupole deformation parameter $\beta_2 = 0.321$ will be determined for the yrast 10^+ state of ^{80}Br from its lifetime datum. In the triaxial deformed case [35], the reduced E2 transitional probability is given

by,

$$B(E2, I \to I-2) = \frac{5}{8\pi} Q_0^2 \frac{(I-1)I}{(2I-1)(2I+1)} \left[\cos(\gamma + 30^\circ) - \cos(\gamma - 30^\circ) \frac{K^2}{(I-1)I} \right]^2, \tag{1}$$

where the Lund convention for γ is used and the intrinsic quadrupole moment

$$Q_0 = \frac{3}{\sqrt{5\pi}} Z R_0^2 \beta_2 (1 + 0.16\beta_2) \tag{2}$$

with the nuclear radius $R_0 = 1.2A^{1/3}$, whereas the projection $K \sim 4$ is adopted here for the yrast band with the $\pi g_{9/2} \otimes \nu g_{9/2}^{-1}$ configuration in ^{80}Br. By this means, the deformation parameters obtained from the triaxial RMF calculations are consistent with the previous performed lifetime measurement in this nucleus [24]. We then adopted these self-consistent RMF deformation parameters as the inputs to the triaxial PRM calculations. The valence nucleon configuration space is expanded in the $1g_{9/2}$ proton subshell and the $1g_{9/2}$ neutron subshell, and the proton and neutron Fermi surfaces for ^{80}Br are placed in the $\pi g_{9/2} 1/2$ and $\nu g_{9/2} 7/2$ orbitals, respectively. The pairing gaps $\Delta_p = 1.295$ MeV and $\Delta_n = 1.287$ MeV are used for protons and neutrons [37]. As demonstrated in Ref. [38], restricting the configuration space to one orbital for the proton and one for the neutron makes the calculated doublet bands to be closer to each other, while larger configuration space is usually more realistic. For the electromagnetic transitions, the gyromagnetic ratios $g_R = Z/A = 0.44$, $g_p = 1.26$, and $g_n = -0.26$ are adopted. The moment of inertia $\Im = 12\ \hbar^2/\text{MeV}$ is adjusted to the experimental energy spectra.

A comparison of the measured and calculated excitation energies $E(I)$ and the energy staggering parameter $S(I)$, defined by $[E(I) - E(I-1)]/2I$, is presented in Fig. 3. One can see that the PRM calculations reproduce the main features of the data well. From Figs. 3(b) and (c), the experimental values of $S(I)$ yield an almost constant value of $\sim$25 keV/$\hbar$, which consists with the expectation for ideal chiral doublet bands [11]. At $I \geq 13\hbar$, the theoretical $S(I)$ values overestimate the amplitude of staggering, which is due to the large Coriolis effect at high spins. The attenuation of Coriolis effect was not taken into account in the present PRM calculations. In Fig. 4, the calculated $B(M1)/B(E2)$ ratios for the doublet bands are compared with experiment. It can be seen that the agreement for the $B(M1)/B(E2)$ ratios at the whole spin region is excellent. This staggering phase of doublet bands in ^{80}Br is similar to the case in the $A \sim$130 mass region with the

$\pi h_{11/2} \otimes \nu h_{11/2}$ configuration, while it is opposite to the case for the $A \sim$100 mass region with the $\pi g_{11/2} \otimes \nu h_{11/2}$ configuration.

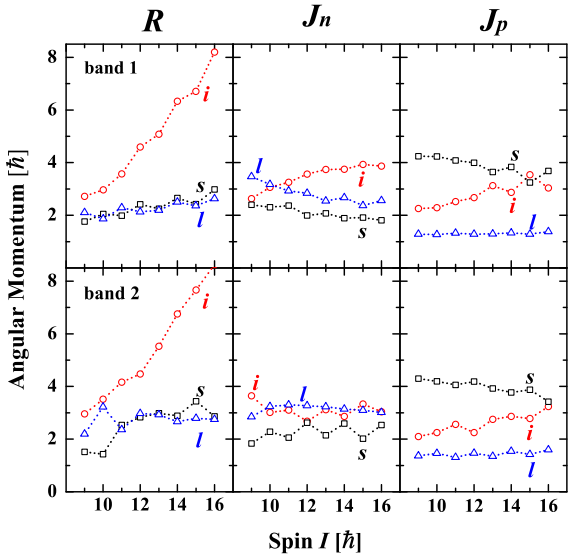

Figure 5: (color online) The root mean square components along the intermediate (i-, circles), short (s-, squares) and long (l-, triangles) axis of the core, valence neutron, and valence protons angular momenta calculated as functions of spin I by means of the PRM for the doublet bands in ^{80}Br.

To exhibit the chiral geometry in ^{80}Br, the expectation values of the squared angular momentum components of the core $R_i = \sqrt{\langle \hat{R}_i^2 \rangle}$, the valence neutron $J_{ni} = \sqrt{\langle \hat{j}_{ni}^2 \rangle}$, and the valence proton $J_{pi} = \sqrt{\langle \hat{j}_{pi}^2 \rangle}$, $(i = l, s, i)$ for the doublet bands are presented in Fig. 5. The collective and valence-proton angular momenta align along the intermediate axis, and the short axis, respectively. For an ideal chiral geometry, the angular momentum of the valence neutron is expected to align along the long axis. As shown in Fig. 5, however, the angular momentum of the hole-like $g_{9/2}$ valence neutron ($g_{9/2}[413]\frac{7}{2}$) in ^{80}Br shows a large mixture between the long and intermediate axes. Therefore, the present coupling pattern of angular momenta somewhat departs from the ideal chiral geometry. However, the total angular momentum is still aplanar.

To give further understanding of the evolution of the chirality with angular momentum [39], the probability distributions for the projection of the total angular momentum along the l-, i- and s-axes are given in Fig. 6 for the

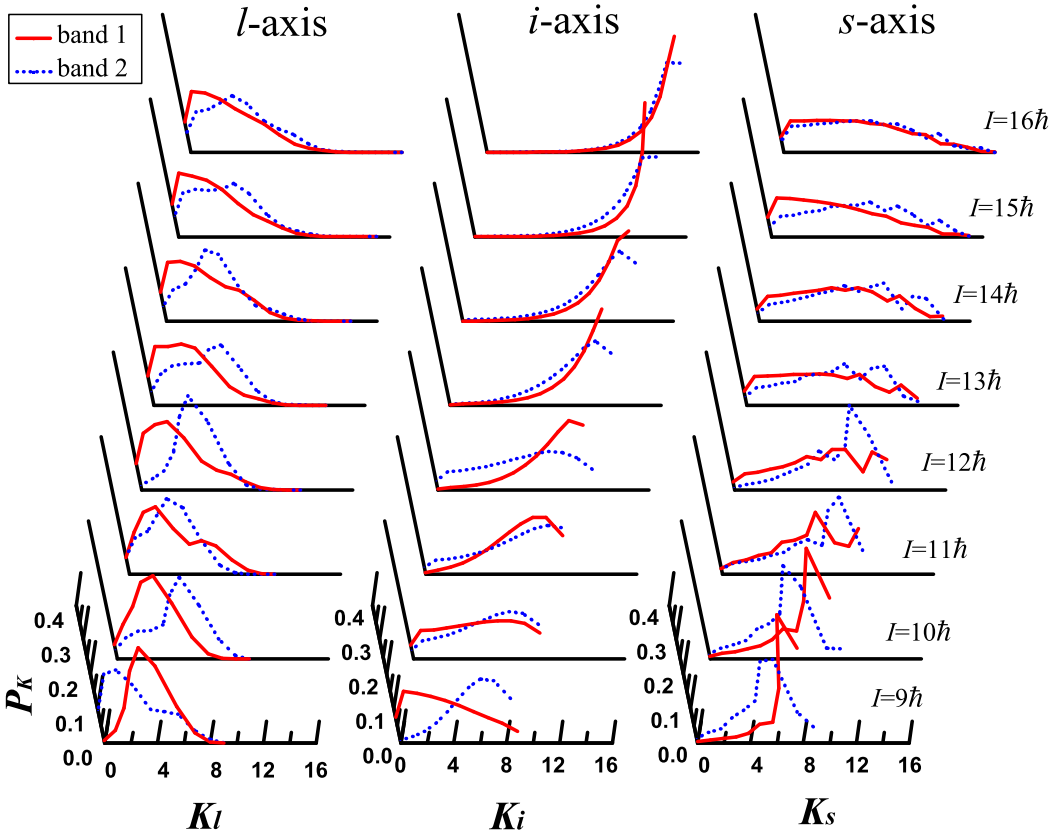

Figure 6: . The probability distributions for projection of total angular momentum on the long (l-), intermediate (i-) and short (s-) axis in PRM for the doublet bands in ^{80}Br.

doublet bands in ^{80}Br. At the bandhead ($I = 9\ \hbar$), the probability distribution of two bands differs as expected for a chiral vibration [39, 40, 41]. For the yrast band the maximum probability for the i-axis appears at $K_i \approx 0$, whereas the probability for the higher band 2 is zero at $K_i \approx 0$, having its peak at $K_i = 6$, which indicates an oscillation of the collective angular momentum vector $\mathbf{R}$ through the s-l-plane. The characteristics of chiral vibration can be found also at other spins, and the pure static chirality which has the identical K distributions for the doublet bands [42] is absent in ^{80}Br. Note that the motion of chiral vibration is mixed by the static chirality for spin $I = 10\ \hbar$, reflected by the fact that the K_i distribution probability in band 1 has a bump for lower K_i, while it is similar as band 2 for higher

K_i [42]. For higher spins, another type of chiral vibration which contains oscillations along both l and s axes can be seen. The lack of static chirality in ^{80}Br should be attributed to the Fermi surface of the neutron placed in the $\nu g_{9/2}[413]\frac{7}{2}$ orbital instead of the top of the $\nu g_{9/2}$ subshell, where less orthogonal coupling is obtained for the angular momenta between the rotor $\mathbf{R}$ and the neutron $\mathbf{J_n}$.

Along the states of band 2 up to spin 13^+, there are several states with the same spin-parity: 11^+ at 2522 keV, 11^+ at 2797 keV, 12^+ at 3473 keV, and 13^+ at 3606 keV (see Fig. 1). These states do not form an obvious collective structure but they are connected with M1/E2 and E2 transitions either to the band 1 or band 2. Moreover, the energies of these states are close to the corresponding states in band 2. These experimental observations suggest that these states may be built on the same configuration with band 2, reflecting the fact that the chiral geometry of ^{80}Br is not very stable. A similar pattern of unstable chiral structure was observed and discussed in ^{132}Cs [9]. These observations are consistent with the K distribution patterns which are shown in Fig. 6, and provide additional support for the interpretation of chiral vibration for the doublet bands in ^{80}Br. The unstable of chiral structure in ^{132}Cs is due to the moderate deformation [9], while the reason in ^{80}Br may come from the fact that the neutron Fermi surface is closer to $\nu g_{9/2}7/2$ orbital than to $\nu g_{9/2}9/2$ orbital.

4. Summary

In summary, excited states of ^{80}Br were investigated by means of in-beam γ-ray spectroscopy. The previously known yrast band has been extended up to I^π=$(16)^+$. A new $\Delta I = 1$ band has been identified which resides $\sim$ 400 keV above the yrast band. The experimental $B(M1)/B(E2)$ ratios extracted for the two bands are comparable in magnitude, and in particular, the ratios for band 1 show clearly the odd-even staggering. By examining the experimental observations against the fingerprints for chirality in Refs. [3, 18], the two bands can be considered as candidates for chiral doublet bands in the $A \sim$80 mass region.

The configuration-fixed constrained triaxial RMF approach is applied to determine quadrupole deformations for the $\pi g_{9/2} \otimes \nu g_{9/2}$ configuration in ^{80}Br. Self-consistent deformation parameters $\beta_2 = 0.346$ and $\gamma = 24.59^\circ$ are obtained. These are favorable deformation parameters for chirality. Using these self-consistent deformation parameters from the RMF approach as in-

put, the present triaxial PRM calculation provides a good description of the positive parity doublet bands in ^{80}Br. The analysis of the probability distributions of the angular momentum indicates that the doublet bands in ^{80}Br might correspond to a typical chiral vibration pattern.

From studies of the odd-odd ^{80}Br nucleus involving the $\pi g_{9/2} \otimes \nu g_{9/2}$ configuration, we have found a new region of chirality. The nucleus ^{80}Br presents mainly the characteristics of chiral vibration. Further efforts are needed to explore nuclear chirality and search for the possible static pattern in this $A \sim 80$ region.

Acknowledgements

This work is supported by the National Natural Science Foundation (Grant Nos. 10775005, 10875002, 10875074, 10947013, 10975007, 10975008, 11005069 and 10710101087), the SA/CHINA research collaboration in science and technology (Grant No. CS05-L06), the Shandong Natural Science Foundation (Grant No. ZR2010AQ005), and the Major State Research Development Programme (No. 2007CB815005) of China, the collaboration between the National Research Foundation of South Africa (NRF, Contract Number UID61851) and the Hungarian National Office for Research and Technology (NKTH, Contract Number ZA-2/2008). One of the authors (K. Juhász) acknowledges support from the TÁMOP 4.2.1./B-09/1/KONV-2010-0007/ IK/IT project, implemented through the New Hungary Development Plan.

We wish to thank the iThemba LABS technical staff and accelerator group for their support and providing the beam.

References

[1] S. Frauendorf and J. Meng, Nucl. Phys. A 617 (1997) 131.

[2] J. Meng, B. Qi, S. Q. Zhang and S.Y. Wang, Mod. Phys. Lett. A 23 (2008) 2560.

[3] J. Meng and S. Q. Zhang, J. Phys. G 37 (2010) 064025.

[4] K. Starosta *et al.*, Phys. Rev. Lett. 86 (2001) 971.

[5] T. Koike, K. Starosta, C. J. Chiara, D. B. Fossan, and D. R. LaFosse, Phys. Rev. C 63 (2001) 061304(R).

[6] R. A. Bark, *et al.*, Nucl. Phys. A 691 (2001) 577.

[7] S. Zhu *et al.*, Phys. Rev. Lett. 91 (2003) 132501.

[8] T. Koike, K. Starosta, C. J. Chiara, D. B. Fossan, and D. R. LaFosse, Phys. Rev. C 67 (2003) 044319.

[9] G. Rainovski *et al.*, Phys. Rev. C 68 (2003) 024318.

[10] S. Y. Wang, Y. Z. Liu, T. Komatsubara, Y. J. Ma, and Y. H. Zhang, Phys. Rev. C 74 (2006) 017302.

[11] C. Vaman, D. B. Fossan, T. Koike, K. Starosta, I. Y. Lee, and A. O. Macchiavelli, Phys. Rev. Lett. 92 (2004) 032501.

[12] P. Joshi *et al.*, Phys. Lett. B 595 (2004) 135.

[13] J. Timar *et al.*, Phys. Rev. C 73 (2006) 011301(R).

[14] D. Tonev *et al.*, Phys. Rev. Lett. 96 (2006) 052501.

[15] C. M. Petrache, G. B. Hagemann, I. Hamamoto and K. Starosta, Phys. Rev. Lett. 96 (2006) 112502.

[16] T. Suzuki *et al.*, Phys. Rev. C 78 (2008) 031302(R).

[17] E. A. Lawrie *et al.*, Phys. Rev. C 78 (2008) 021305(R).

[18] S. Y. Wang, S. Q. Zhang, B. Qi, and J. Meng, Chin. Phys. Lett. 24 (2007) 664.

[19] V.I. Dimitrov, S. Frauendorf, and F. Dönau, Phys. Rev. Lett. 84 (2000) 5732.

[20] J. F. Sharpey-Schafer, Nucl. Phys. News 14 (2004) 5.

[21] F. S. Komati *et al.*, AIP Conf. Proc. 802 (2005) 215.

[22] J. Eberth, Prog. Part. Nucl. Phys. 28 (1992) 495.

[23] R. Schwengner *et al.*, Phys. Rev. C 65 (2002) 044326.

[24] I. Ray, P. Banerjee, S. Bhattacharya, M. Saha-Sarkar, S. Muralithar, R. P. Singh and R. K. Bhowmik, Nucl. Phys. A 678 (2000) 258.

[25] Y. Zheng *et al.*, J. Phys. G 30 (2004) 465.

[26] R. Schwengner *et al.*, Z. Phys. A 326 (1987) 287.

[27] J. C. Wells *et al.*, Phys. Rev. C 22 (1980) 3.

[28] J. Meng, J. Peng, S.Q. Zhang and S.G. Zhou, Phys. Rev. C 73 (2006) 037303.

[29] S. Y. Wang, S. Q. Zhang, B. Qi, and J. Meng, Phys. Rev. C 75 (2007) 024309.

[30] S. Q. Zhang, B. Qi, S. Y. Wang, and J. Meng, Phys. Rev. C 75 (2007) 044307.

[31] S. Y. Wang, S. Q. Zhang, B. Qi, J. Peng, J. M. Yao, and J. Meng, Phys. Rev. C 77 (2008) 034314.

[32] W. H. Long, J. Meng, N. VanGiai, and S. G. Zhou, Phys. Rev. C 69 (2004) 034319.

[33] S.G. Buccino, F.E. Durham, J.W. Holcomb, T.D. Johnson, P.D. Cottle, S.L. Tabor, Phys. Rev. C 41 (1990) 2056.

[34] R. Loritz, O. Iordanov, E. Galindo, A. Jungclaus, D. Kast, K.P. Lieb, C. Teich, F. Cristancho, Ch. Ender, T. Hätlein, F. Köck, D. Schwalm, Eur. Phys. J. A 6 (1999) 257.

[35] P. Petkov *et al.*, Nucl. Phys. A 640 (1998) 293.

[36] K. Andgren *et al.*, Phys. Rev. C 71 (2005) 014312.

[37] P. Möller, J. R. Nix, W. D. Myers, and W. J. Swiatecki, Atomic Data Nucl. Data Tables 59 (1995) 185.

[38] E.A. Lawrie and O. Shirinda, Phys. Lett. B 689 (2010) 66.

[39] B. Qi, S. Q. Zhang, J. Meng, and S. Frauendorf, Phys. Lett. B 675 (2009) 175.

[40] S. Mukhopadhyay *et al.*, Phys. Rev. Lett. 99 (2007) 172501.

[41] S. Y. Wang, B. Qi, and D. P. Sun, Phys. Rev. C 82 (2010) 027303.

[42] B. Qi, S. Q. Zhang, S. Y. Wang, J.M. Yao and J. Meng, Phys. Rev. C 79 (2009) 041302(R).